Desalination and Water Treatment
www.deswater.com

doi: 10.1080/19443994.2013.801796

52 (2014) 3122–3132
April

Taylor & Francis
Taylor & Francis Group

Removal of chromium(VI) from waste water by using adsorbent prepared from green coconut shell

S. Kumar[a], B. C. Meikap[a,b,*]

[a]*Department of Chemical Engineering, Indian Institute of Technology (IIT), Kharagpur, West Bengal 721302, India*
Tel. +913222283958; email: bcmeikap@che.iitkgp.ernet.in
[b]*Department of Chemical Engineering, School of Engineering, Faculty of Engineering, Howard College Campus, University of KwaZulu-Natal, King George V. Avenue, Durban 4041, South Africa*

Received 20 March 2013; Accepted 22 April 2013

ABSTRACT

In recent years, industrial effluents containing heavy metals have become a major problem. For the removal of heavy metals, several types of adsorbents have been developed economically from waste materials by different processes. In present work, "Green Coconut Shell," which is waste material, was chosen for the development of adsorbent by treatment with orthophosphoric acid economically. This adsorbent was used for the removal of chromium (VI) in batch mode in concentration and temperature range of 10–100 mg/g and 10–80°C, respectively. The influence of contact time, temperature, concentration, adsorbent dose, particle size, and pH was studied. Langmuir and Freundlich isotherm models were fitted for equilibrium data with maximum adsorption capacity of 22.96 mg/g. Pseudo-second-order model also confirmed that the chromium(VI) uptake capacity of adsorbent was due to pore, film, and particle diffusion. To know the properties of adsorbent different analysis such as XRF, X-ray diffraction, scanning electron microscope, energy dispersive spectroscope, and particle size distribution using Malvern analyzer were studied. The adsorption capacity of green coconut shell-based adsorbent achieved was greater than 90% for 10 mg/l solution and contact time of 30 min.

Keywords: Green coconut shell; Orthophosphoric acid; Adsorption; Concentration; Chemical activation; Hexavalent; Contact time

1. Introduction

The problems of the ecosystem are increasing with developing technology. Heavy metals pollution is one of the major problems. Therefore, the earth's water may contain various toxic metals. Drinking water is obtained from springs which may be contaminated by various toxic metals. The water contamination with heavy metal ions is a very severe problem all over the World [1–2]. So the motto of the present study was to develop the adsorbent from "Green Coconut Shell" economically, which should have best efficiency towards the removal of heavy metals from industrial effluent. The effect of various parameters that affect adsorption viz. Contact time, initial concentration, particle size, temperature, pH, and adsorbent dose were performed in batch experiment. To know the heavy

---

*Corresponding author.

metals uptake capacity, the physical and chemical properties of the adsorbent was studied by proximate, X-ray diffraction (XRD), XRF, scanning electron microscope (SEM), energy dispersive spectroscopic (EDS), and Malvern particle size analysis. It was tried to fit the equilibrium data in different models such as Lagergren, Pseudo-second-order, Webber and Morris, Langmuir, and Freundlich models.

Chromium(VI) is considered as a high-priority environmental pollutant and it is widespread in metal finishing, lather tanning, electroplating, textile industries, and chromate preparation. In aqueous phase, chromium mostly exists in two oxidation states, namely, trivalent chromium and hexavalent chromium [3–7]. Generally, most of the hexavalent compounds are toxic, carcinogenic, and mutagenic while trivalent chromium is essential for humans and is very less toxic. For example, it was reported that $Cr_2O_7^{2-}$ causes lung cancer. The International agency for research on cancer has determined that Cr(VI) is carcinogenic to humans. Therefore, the world health organization recommends the toxic limits of Cr(VI) in drinking water at the level of 0.05 mg/L.

Conventional techniques for Cr(VI) removal from aqueous solution include chemical reduction, chemical precipitation, ion exchange, membrane separation, and adsorption [8–11]. In application of the method of adsorption, the most widely used adsorbent is activated carbon because it has relatively higher surface area. But the production of commercial activated carbon is still an expensive process. Literature survey reveals that there are several processes to prepare the activated carbon that are used to remove various heavy metal pollutants [12–16]. However, it still remains a big challenge to search an effective adsorbent.

2. Materials and methods

2.1. Selection of adsorbent

Adsorbents are nonhazardous processed carbonaceous products having a porous structure and a large internal surface area. These materials can absorb a wide variety of substances i.e. they are able to attract molecules to their internal surface. Therefore, it is called an adsorbent. The volume of pores of the activated carbon is generally greater than 0.2 ml/g. The internal surface area is generally greater than 400 m^2/g. The adsorbent prepared from green coconut shell is still an excellent adsorbent for many toxic materials present in the various types of waste water. Adsorbent should be uniform in size and contain less ash and high volatile matter. This ability to arrest the different pollutant molecules is mainly attributed to its higher specific surface area.

2.2. Preparation of adsorbent

The green coconut was collected from tech market of IIT Kharagpur, West Bengal and cut in small pieces. Then, it was dried in an oven at 110˚C for removing moisture. After moisture removal, the sample was crushed using hammer and is finally changed to 3–5 mm size by using ball mill. Then, the green coconut shell powder was treated with ortho phosphoric acid (H_3PO_4) in 4/5 (g/ml) ratio. This mixture was then left to react for 1–2 h and then heated in the electric furnace at a temperature of 400–600˚C for 1.5 h. After that it was cooled and washed with distilled water, and dried in oven at 110˚C for 24 h and finally, the adsorbent was ready for use.

2.3. Loss of weight during active

Weight loss during activation was conducted at temperature 300 and 600˚C with time. From graph, it is clear that at 300˚C, the maximum weight loss is around 35% and at 600˚C, the loss is around 84%. For both temperatures, initially, the rate of weight loss is high, then gradually decreases, and after some time, becomes nearly constant (Fig. 1).

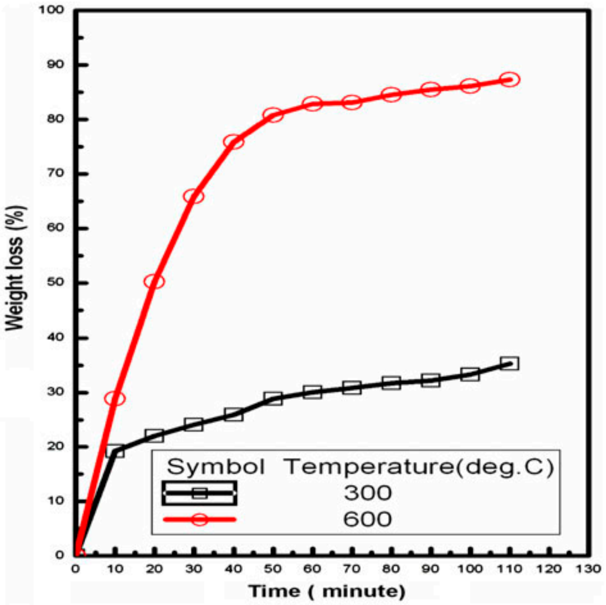

Fig. 1. Weight loss (%) at temperature 300 and 600˚C during activation.

2.4. Materials used in experiment

Different types of materials such as filter paper, conical flask, volumetric flask, pH meter, and Potassium dichromate ($K_2Cr_2O_7$), Orthophosphoric acid (H_3PO_4), Sodium hydroxide (NaOH) and Nitric acid (HNO_3) chemicals were used in experiment.

3. Experimental study

3.1. Experimental equipments

3.1.1. Furnace

It is an equipment which is used for heating. Generally, furnace is used for very high temperature. At present, electric furnace was used during the preparation of activated carbon from green coconut shell in absence of air. The furnace is primarily split into three sections—the *shell*, which consists of the sidewalls and lower steel bowl, the *hearth*, which consists of the refractory that lines the lower bow, the *roof*, which may be refractory-lined or water-cooled.

3.1.2. Shaker

It is made of double-walled, inner chamber made of stainless steel and outer chamber made of mild steel sheet finished with powder-coating paint. In lab, a shaker with BOD incubator is available, commercially available in different shapes. In the present paper, this equipment was used for shaking purpose at different temperatures and shaking frequencies. It is highly insulated with high-grade glass–wool and there is an air circulation fan to maintain uniform temperature. The temperature is controlled by a digital temperature indicator-cum-controller and can operate up to a temperature of 600°C.

3.1.3. Atomic absorption spectroscopy

Atomic absorption spectroscopy (AAS) uses the absorption of light to measure the concentration of gas phase atoms. Since the samples are usually liquids or solids, the analyte atoms or ions must be vaporized in a flame or graphite furnace. The atoms absorb ultraviolet or visible light and make transitions to higher electronic energy levels. The analyte concentration is determined from the amount of absorption. Applying the Beer–Lambert law directly in AAS is difficult due to variation in the atomization efficiency from the sample matrix and the nonuniformity of concentration and path length of the analyte atoms. Concentration measurements are usually determined from a working curve after calibrating the instrument with standards of known concentration.

3.2. Preparation of stock solution of $K_2Cr_2O_7$

Stock solution of $K_2Cr_2O_7$ was prepared by mixing 2.8289 g with 1,000 ml distilled water in a volumetric flask and then from stock solution, concentrated solution is prepared as reported by Acharya et al. [1].

3.3. Experimental procedure

Stock solution of $K_2Cr_2O_7$ was prepared and from stock solution, different concentrations of $K_2Cr_2O_7$ prepared. Certain quantity of activated carbon and concentrated solution of $K_2Cr_2O_7$ were put in a conical flask and placed in shaker. After certain time, the solution was filtered and lastly, the final concentration was measured with the help of AAS analysis.

3.4. Characterization of green coconut shell powder

3.4.1. XRF analysis

Table 1
Green coconut shell before and after activation

S.N	Elements	Conc. (%) of green coconut shell (after activation)	Conc. (%) of green coconut shell (before activation)
1	Na	0.193	1.83
2	Mg	0.401	3.17
3	Al	1.44	1.93
4	Si	6.33	1.87
5	P	82.4	3.03
6	S	1.31	1.96
7	Cl	0.801	23.9
8	K	4.1	37.7
9	Ca	1.25	7.97
10	Ti	0.184	0.487
11	Fe	1.05	8.23
12	Ni	0.098	0.24
13	Cu	0.077	0.106
14	Zn	0.060	0.26
15	Sr	0.163	0.562
16	Jr	0.030	0.114
17	Pb	0.080	0.118
18	Br	0	0.165
19	Mn	0	0.124

Table 2
Result of XRD analysis of green coconut shell powder before activation

Ref. code	Peak position ($^0 2\theta$)	Comp. name	Crystal system	Color	*h*	*k*	*l*	d(*A*)
46-1045	94.78	Quartz (SiO_2)	Hexagonal	White	1	0	1	3.34347
33-1161	61.14	Quartz (SiO_2)	Hexagonal	Colorless	1	0	1	3.342
27-1402	88.07	Silicon (Si)	Cubic	Gray	1	1	1	3.1355
33-0664	40.59	Hematite (Fe_2O_3)	Rhombohedral	Dark reddish brown	1	0	4	2.7
05-0586	73.78	Calcite ($CaCO_3$)	Rhombohedral	Colorless	1	0	4	3.035
35-0816	58.71	Fluorite (CaF_2)	Cubic	Colorless	2	2	0	1.9316

Table 3
Result of XRD analysis of green coconut shell powder after activation

Ref. code	Peak position	Comp. name	Crystal system	Color	*h*	*k*	*l*	d(*A*)
46-1045	60,68	Quartz (SiO_2)	Hexagonal	White	1	0	1	3.34347
73-1667	68.14	Bornite (Cu_5FeS_4)	Cubic	–	2	2	0	1.93394
06-0694	81.46	Chromium (Cr)	Cubic	Gray mettalic	1	1	0	2.03900
33-1161	50.14	Quaetz (SiO_2)	Hexagonal	Colorless	1	0	1	3.34200
05-0586	81.46	Calcite ($CaCO_3$)	Rhombohedral	Colorless	1	0	4	3.035
75-0134	68.14	Uranium oxide (Uo_2)	Cubic	–	1	1	1	3.15753

3.4.2. XRD analysis

The XRD analysis was done using "Panalytical High Resolution XRD-I, PW 3040/60" to know the crystalline structure of green coconut shell powder before and after activation (Tables 2 and 3). From both tables, it can be concluded that there is a little change in crystalline structure of the sample before and after activation, which may be due to the reason that treatment was done at temperature around 350˚C and the pore structure changed due to change in the textural properties of samples.

3.4.3. SEM and EDS analyses

The microstructural details and compositional analysis of green coconut shell powder was determined by "Jeol JSM5800 SEM with Oxford EDS Detector" as shown in figures given below and the microscope has a tungsten filament and a maximum acceleration voltage of 30 kV. The surface structure of green coconut shell was analyzed by SEM at 1.00KX magnification. The micrograph and composition of Untreated and treated green coconut shell powder were analyzed

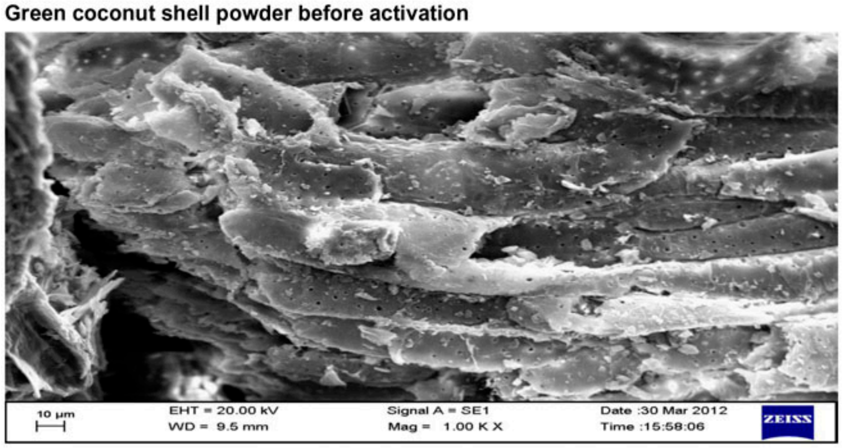

Fig. 2. Scanning electron micrograph of green coconut shell powder before activation.

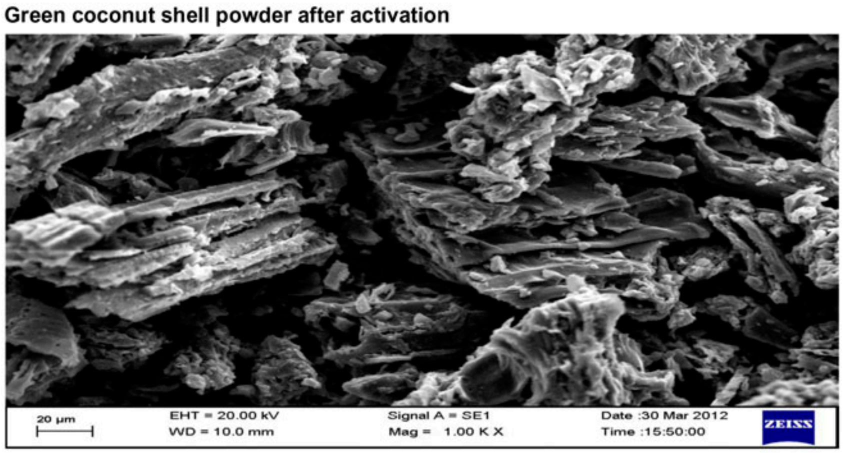

Fig. 3. Scanning electron micrograph of coconut shell activated powder before Cr(VI) adsorption.

Table 4
EDS analysis

S. N	Elements	Weight %	
		Before activation	After activation
1	C	58.89	39.51
2	O	38.71	46.97
3	Cl	0.68	0
4	Si	0	0.58
5	K	1.72	12.93

by SEM and EDS analyzer as shown in Figs. 2 and 3, respectively.

It was observed that the pores of the untreated green coconut shell were closed before activation as shown in Fig. 2. The activated green coconut shell had a porous structure showing large number of pores and larger size of pores indicating a large surface area as shown in Fig. 3.

Fig. 2 shows that the material is irregular and porous. This surface characteristic would substantiate high adsorption through mass transport inside the sorbent. Table 4 presents EDS analysis, and it shows the presence of C, O, Si, P, Cl, K as natural species and the presence of these elements could have an effect on adsorption mechanism. Figs. 2 and 3 show significant difference between the surface before and after activation and the reason attributed was that a high percent of voids are being occupied by the volatile matters.

3.4.4. Particle size analysis

Malvern instrument "Mastersizer 2000" was used for the analysis of green coconut shell powder before and after activation and was compared with commercial activated carbon. The samples were dispersed in water with the help of an ultrasonic magnetic stirrer before feeding into the instrument. By the use of laser

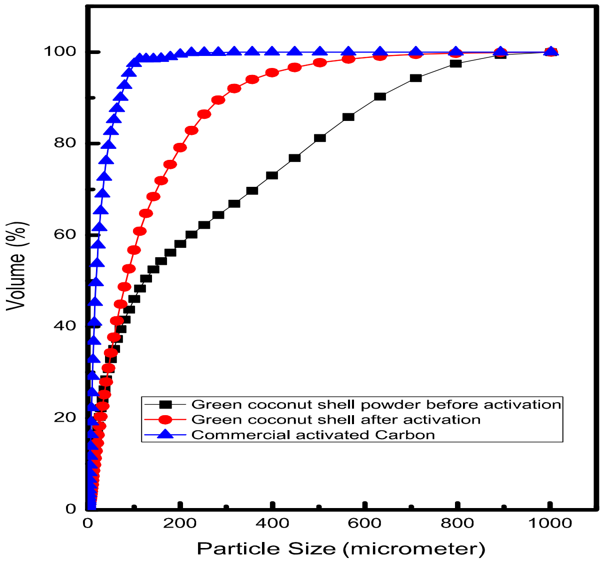

Fig. 4. Particle size analysis graph of green coconut shell powder before and after activation and comparison with commercial activated Carbon.

Table 5
Physical properties of green coconut shell-activated powder

Moisture content	3.02%
Ash percentage	6.65%
Volatile matter	36.50%
Fixed carbon	53.83%

diffraction technology, the technique of laser diffraction based around the principle that particles passing through a laser beam will scatter light at an angle which is directly related to particle size. Scattering angle increases logarithmically when particle size decreases. From Fig. 4, it can be seen that as particle size increases, cumulative volume percentage also increases and reaches maximum around 900 µm. The properties of green coconut shell powder are given in Table 5.

4. Results and discussion

4.1. Effect of contact time

The relationship between contact time and chromium adsorption at different initial chromium concentrations is shown below. The adsorption was very fast from the beginning to 20 min and the adsorption capacities increased from 25 to 94% with the chromium concentration range of 10–100 mg/l at a contact time of 30 min. With further increase of time, the adsorption kinetics decreased progressively, and finally, the adsorption approached to equilibrium within 40 min in all the cases. The fast adsorption at the initial stage is probably due to the increased number of vacant sites available in the beginning. The progressive increase in adsorption and consequently, the attainment of equilibrium adsorption may be due to limited mass transfer of the adsorbate molecules from the bulk liquid to the external surface of adsorbent initially and subsequently, by slower internal mass transfer within the internal particles (Fig. 5).

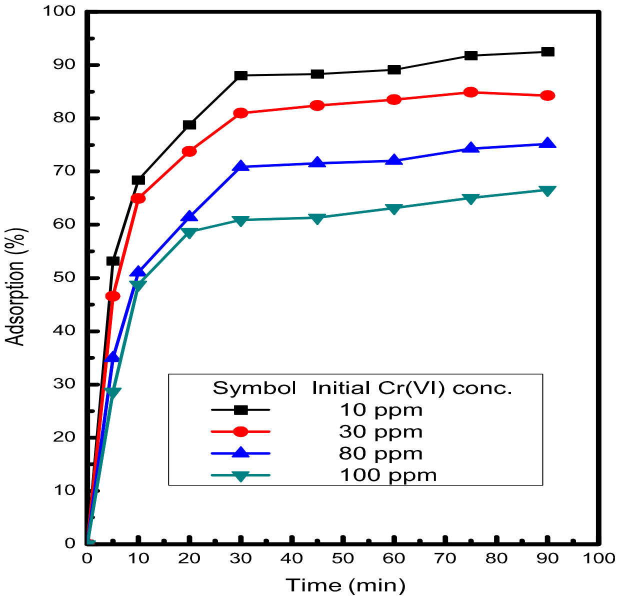

Fig. 5. Effect of contact time on adsorption of chromium (VI) at different initial feed concentrations, constant adsorbent dose 5 g/l and at constant temperature 30°C and pH 6.5.

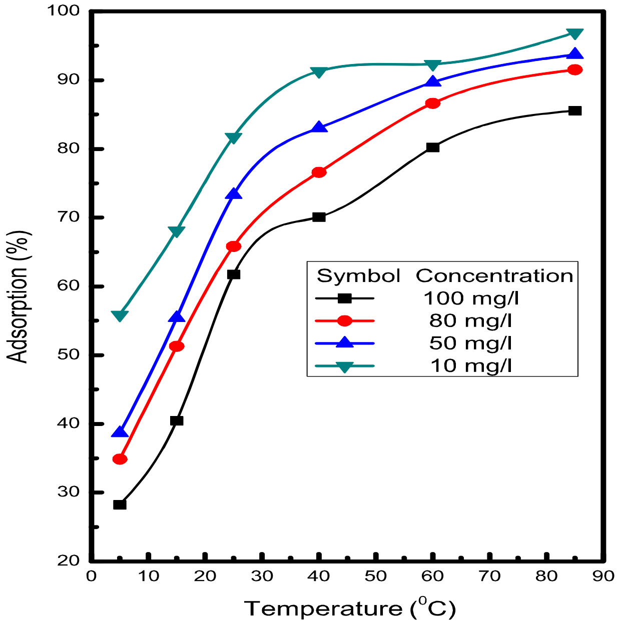

Fig. 6. Effect of temperature for different initial feed concentrations at constant adsorbent dose 5 g/l and pH 6.5 and at different concentrations.

4.2. Effect of temperature

The temperature has great effects on the adsorption process. An increase in temperature is known to increase the diffusion rate of the adsorbate molecules across the external boundary layer and within the pores. Furthermore, changing the temperature will modify the equilibrium capacity of the adsorbent for a particular adsorbate. The experiments were performed for different temperatures of 5, 15, 25, 40, 60, and 85°C at constant adsorbent doses of 5 g/l, constant pH of 6.5, and initial feed concentrations of 10, 50, 80, and 100 mg/l. Fig. 6 shows that the percentage adsorption increases as the temperature increases for activated green coconut shell powder and reaches maximum of about 95% for a concentration of 10 mg/l. For temperature 40–60°C, the rate of adsorption is maximum and after 60°C, the rate becomes nearly constant i.e. equilibrium is achieved. As temperature increases, adsorption increases, so the process is endothermic in nature.

4.3. Effect of adsorbent doses

The experiment was performed for adsorbent doses of 2, 4, 6, 8, and 10 g/l for a constant

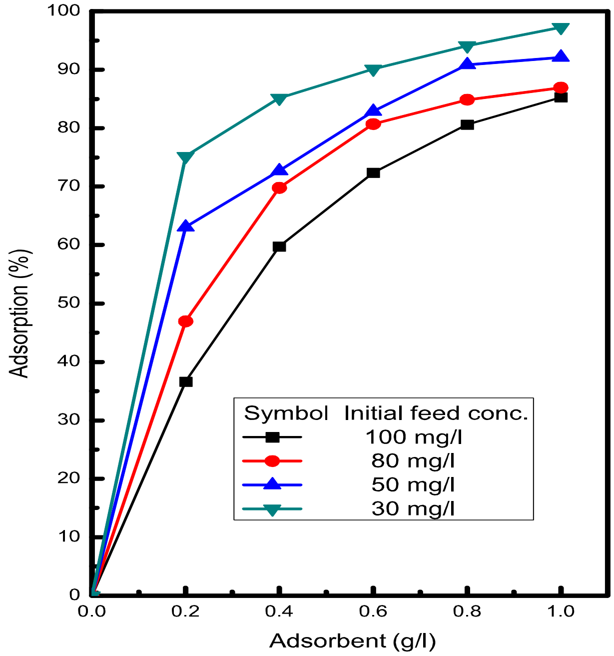

Fig. 7. Effect of adsorbent doses on adsorption of chromium(VI) at different initial feed concentrations and at constant temperature 30˚C.

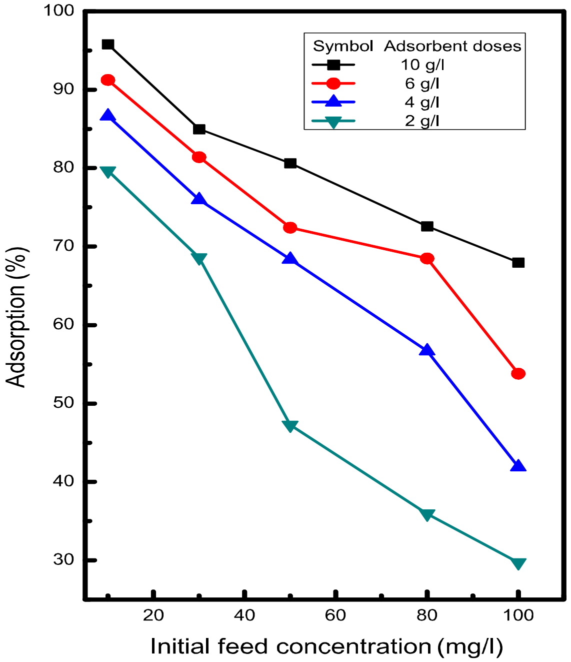

Fig. 8. Effect of initial feed concentration on adsorption of chromium(VI) at different adsorbent doses and at constant temperature 30˚C and pH 6.5.

temperature of 30˚C and contact time of 30 min at pH of 6.5. The effect of adsorbent dosage on the percentage removal of chromium(VI) has been shown in Fig. 7. It can be seen from the figure that initially the percentage removal increases very sharply with the increase in adsorbent dosage, but beyond a certain value 0.2–0.8 g, the percentage removal reaches almost a constant value. This trend is expected because as the adsorbent dose increases, the number adsorbent particles increases and, thus, more chromium(VI) is attached to their surfaces. The adsorption capacities for chromium(VI) increased from 75 to 96%, 62 to 90%, 45 to 82% and 35 to 75% at 30, 50, 80, and 100 mg/l initial feed concentrations with adsorbent doses, respectively.

4.4. Effect of concentration

The experiment was performed for different initial feed concentration of 10, 30, 50, 80, and 100 mg/l at a constant pH of 6.5 for adsorbent doses of 2, 4, 6, and 10 g/l. The effect of chromium concentration in the solution on the adsorption has been shown in Fig. 8. It can be seen from the figure that with increased initial feed concentration of chromium(VI), there was a decrease in the percentage of adsorption of chromium. The adsorption capacities for chromium(VI) decreased from 80 to 30%, 85 to 42%, 91 to 56%, and 96 to 70% at adsorbent doses 2, 4, 6, and 10 g/l, respectively, with the increase in the initial feed concentrations from 10 to 100 mg/l.

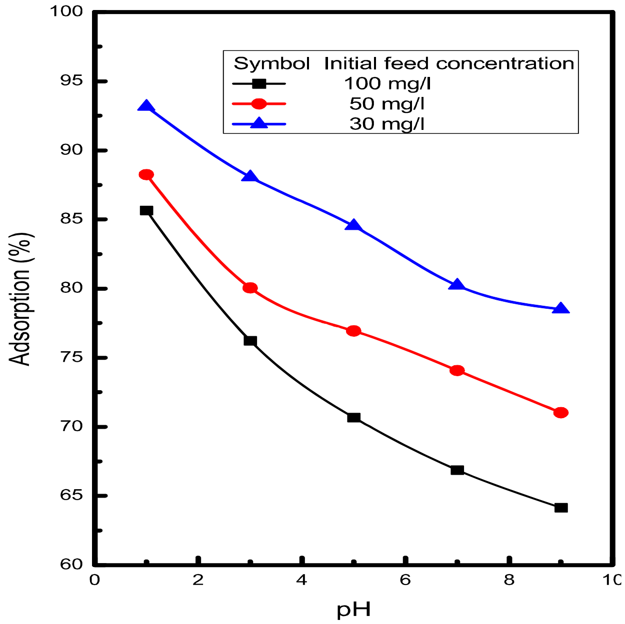

Fig. 9. Effect of PH on adsorption of chromium(VI) at same adsorbent doses and at constant temperature 28˚C.

4.5. *Effect of pH*

The effect of pH is an important parameter for the adsorption of heavy metals from waste water. The experiment was performed for different levels of initial pH of 1, 3, 5, 7, and 9 for initial feed concentrations of 30, 50, and 100 mg/l and at constant adsorbent dose of 5 g/l. The temperature was maintained at 28℃ and contact time of 30 min. From Fig. 9, it is clear that the adsorption increases from 78 to 93%, 72 to 88%, and 55 to 81% for concentration of 30, 50, and 100 mg/l and maximum adsorption takes place at pH 1 and hence the process will be favorable in a highly acidic medium.

4.6. *Effect of particle size*

The effect of particle size is another important parameter for the adsorption of heavy metals from waste water. The experiment was performed for different particles of 30, 60, and 110 mm mesh size for an initial feed concentration range of 10–100 mg/l and at constant adsorbent dose of 5 g/l. The temperature was maintained at 28℃ and contact time of 30 min. From Fig. 10, it is clear that adsorption increases from 30 to 73%, 45 to 84%, and 60 to 95% for particles of 30, 60, and 110 mm mesh size.

4.7. *Kinetics study for removal of Cr(VI) using adsorbent prepared from green coconut shell*

4.7.1. *Lagergren model (pseudo-first-order model for Cr(VI) adsorption)*

The rate constant of adsorption was calculated using the Lagergren's first-order kinetic Eq. (1).

$$\log(q_e - q) = \log q_e - (K_{ad}/2.303)t \tag{1}$$

where q and q_e are the amount of Cr(VI) adsorbed (mg/g) at time t (min), and at equilibrium time and K_{ad} is the equilibrium rate constant of pseudo-first-order adsorption (min^{-1}). The linear plot obtained by plotting log $(q_e - q)$ vs time "t" shows the validity of Lagergren first-order kinetic equation for the adsorption of Cr (VI).

4.7.2. *Pseudo-second-order model for Cr(VI) adsorption*

The adsorption kinetics can also be described by a pseudo-second-order reaction. The linearized integral form of the model is given in Eq. (2)

$$t/q = 1/k_2 q_e^2 + (1/q_e t) \tag{2}$$

where k_2 is the rate constant of pseudo-second-order rate adsorption. This model can be applied by linear

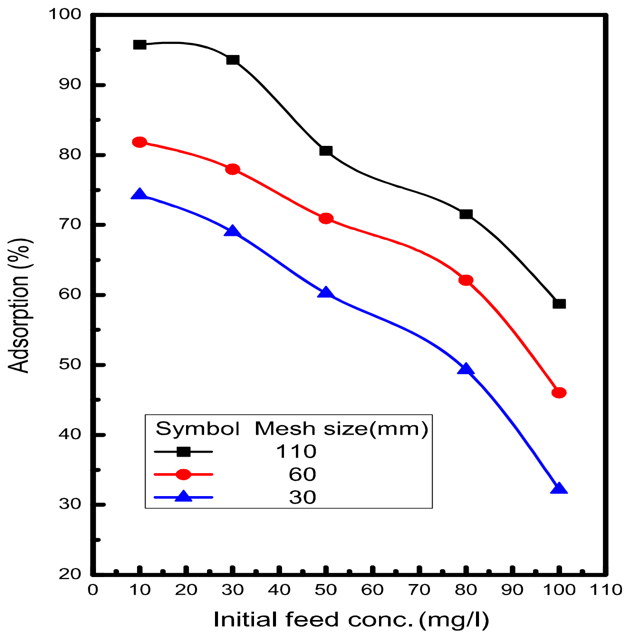

Fig. 10. Effect of particle size on adsorption of chromium(VI) at same adsorbent dose of 5 g/l, pH 6.5 and at constant temperature 28℃.

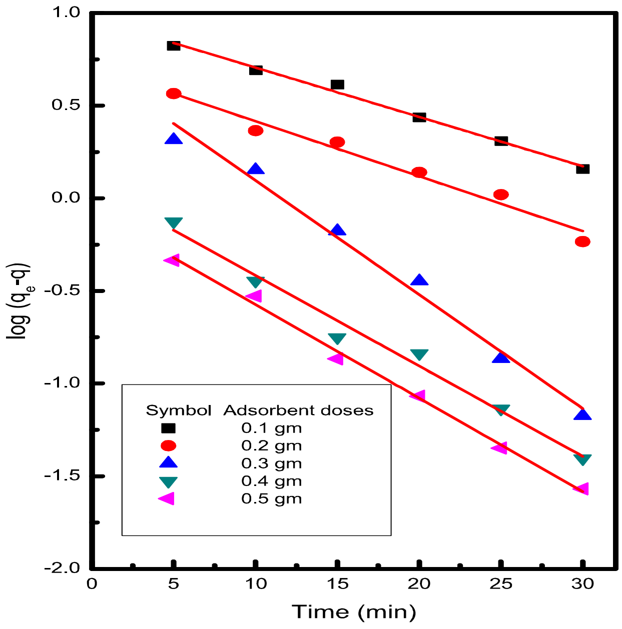

Fig. 11. Kinetics of Cr(VI) removal according to Lagergren model at feed doses of 1, 2, 3, 4, and 5 g/l.

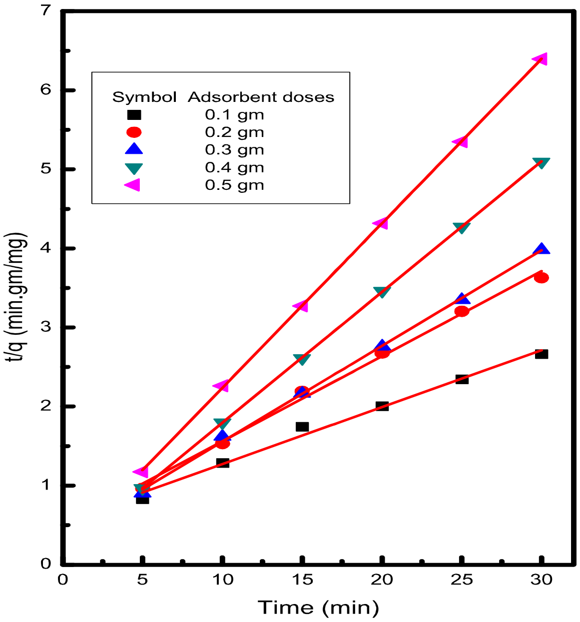

Fig. 12. Kinetics of Cr(VI) removal according to Lagergren model at feed doses of 1, 2, 3, 4, and 5 g/l.

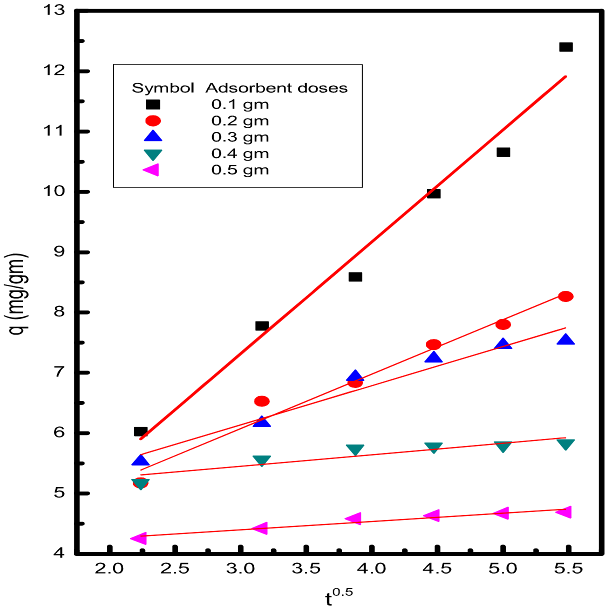

Fig. 13. Kinetics of Cr(VI) removal according to Webber and Morris model at feed doses of 1, 2, 3, 4, and 5 g/l.

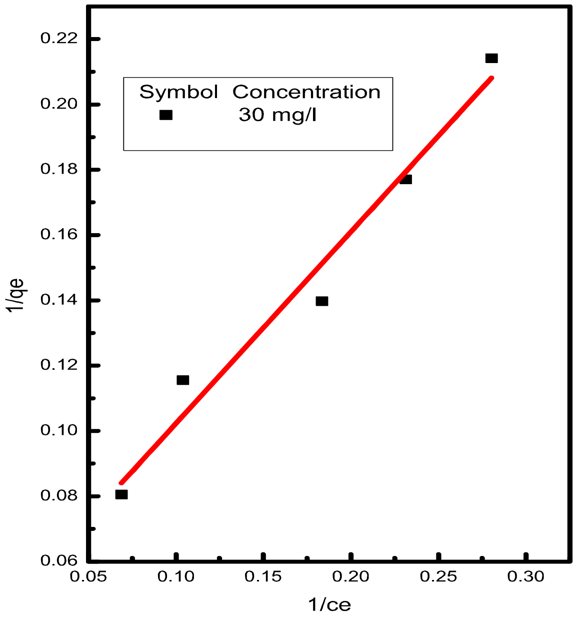

Fig. 14. Kinetics of Cr(VI) removal according to Langmuir Isotherm model at initial feed concentration of 30 mg/l.

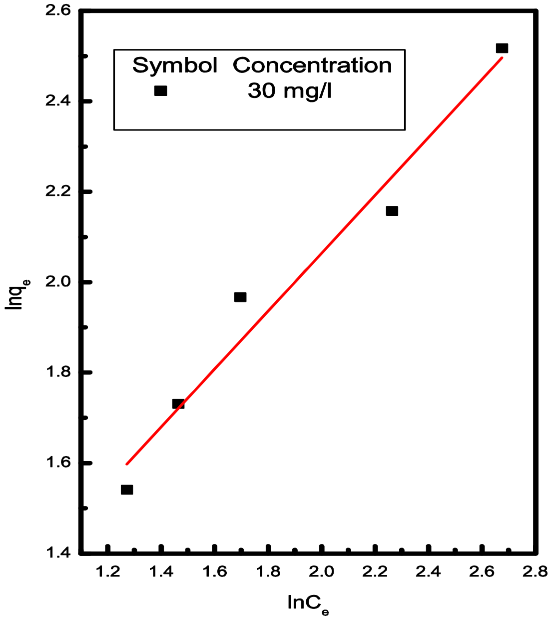

Fig. 15. Kinetics of Cr(VI) removal according to Freundlich Isotherm model at initial feed concentration of 30 mg/l.

plot of (t/q) vs. t for adsorption kinetics of Cr(VI) and is presented in Fig. 24.

The applicability of two models can be studied by each linear plot in Figs. 11 and 12. To know the applicability of each model, the correlation coefficient R^2 was calculated for every sample from these plots. The values of R^2 for Lagergren model (pseudo-first-order) and pseudo-second-order reaction for adsorbent doses 1, 2, 3, 4, and 5 g/l was calculated in the range of 0.96902–0.995 and 0.9877–0.9999. Here, the correlation coefficient of pseudo-second-order model is greater than pseudo-first-order model which shows that the given data for chemisorption mechanism fitted better

Table 6
Adsorption isotherms parameter at pH 2.5 and temperature 28°C for chromium(VI) removal

Parameters	q_m (mg/g)	K_L (l/g)	R^2		K_F (l/g)	n
Values	22.9621	0.0742	0.9624	Langmuir	2.1862	1.5606
			0.9557	Freundlich		

for pseudo-second-order than pseudo-first-order model.

4.7.3. Webber and Morris model

In the case of liquid adsorption, intraparticle diffusion model is important because it is rate-determining step. During the batch mode of operation there is a possibility of the transport of sorbate species into the pores of sorbent which is often the rate-controlling step. The rate constant (k_{id}) of intraparticle diffusion was determined using equation:

$$q = k_{id} t^{0.5} \tag{3}$$

where q is the quantity adsorbed (mg/g) at time t and $t^{0.5}$ is the square root of time.

The graph was plotted for adsorbent doses of 1, 2, 3, 4 and 5 g/l and the values of k_{id} was calculated as 1.85448, 0.90282, 0.64938, 0.19053 and 0.13781, respectively, at a constant pH of 2. Initially, the adsorption was due to boundary-layer diffusion and in later, due to intraparticle diffusion. The correlation coefficients for different doses was found, 0.97333, 0.96846, 0.94608, 0.79266, and 0.92475 which shows that intraparticle diffusion was not the only rate-controlling step because it does not pass through origin.

4.7.4. Langmuir isotherm model

The theoretical Langmuir isotherm equation can be represented as

$$q_e = \frac{q_m K_L C_e}{1 + K_L C_e} \tag{4}$$

where K_L is the Langmuir constant related to the energy of adsorption (l/mg) and q_m is the maximum amount of adsorption corresponding to complete monolayer coverage on the surface (mg/g). The constants K_L and q_m can be determined from the following linearized form Eq. (4) of

$$\frac{1}{q_e} = \frac{1}{q_m} + \frac{1}{K_L q_m} \frac{1}{C_e} \tag{5}$$

The essential features of Langmuir adsorption isotherm can be expressed in terms of a dimensionless constant called the separation factor or equilibrium parameter (R_L). Conformation of the experimental data into Langmuir isotherm model indicates the homogeneous nature of the activated carbon alumina surface.

4.7.5. Freundlich isotherm model

The Freundlich isotherm can be used for nonideal sorption that involves heterogeneous surface energy systems and is expressed by the following equation:

$$q_e = K_F C_e^{\frac{1}{n}} \tag{6}$$

where K_F is a rough indicator of the adsorption capacity and $1/n$ is the adsorption intensity. In general, as the K_F value increases, the adsorption capacity of an adsorbent for a given adsorbate increases. Eq. (6) may be linearized by taking logarithms:

$$\log q_e = \log K_F + \frac{1}{n} \log C_e \tag{7}$$

Multicomponent equilibrium studies have been developed attaining different perspectives.

Langmuir and Freundlich models are plotted in the form of Figs. 14 and 15 and values are presented in Table 6. It can be seen from graph that the isotherm data fits the Langmuir equation well ($R^2 = 0.9624$). The value of K_L and q_m were determined from the figure and were found to be 0.0742 l/g and 22.9621 mg/g, respectively. The isotherm data also fits the Freundlich equation well ($R^2 = 0.9557$). The values of K_F and n were found to be 2.1862 l/g and 1.5606, respectively, at a pH of 2.5 for maximum adsorption.

5. Conclusions

For the removal of chromium(VI) from aq. solution, several adsorbents were used but the adsorbent prepared from unwanted green coconut shell is an effective and low-cost adsorbent for the removal of Cr(VI) from waste water. Conclusions of the present study are given below:

- The different properties of green coconut shell powder before and after activation was analyzed by proximate analysis, XRF, XRD, SEM, EDS, and Malvern particle size analysis.

- The effect of contact time can be conclude from Fig. 5. At equilibrium, the percentage removal of Cr(VI) is 94% for 10 mg/l and it reduces to 65% as the concentration increases to 100 mg/l. As contact time increases, the percentage adsorption also increases but after 30–40 min, the concentration becomes nearly constant which indicates that an equilibrium is achieved.
- The effect of temperature is shown in Fig. 6 for concentrations of 10, 50, 80, and 100 mg/l. Initially the percentage adsorption of Cr(VI) increases with increase in temperature and becomes nearly constant after 60°C and the maximum adsorption was around 95% for 10 mg/l and minimum around 80% for 100 mg/l.
- The effect of adsorbent dose is shown in Fig. 7 for concentrations of 30, 50, 80, and 100 mg/l. From graph, it can be seen that as adsorbent dose increases from 2 to 10 g/l, the percentage adsorption also increases and maximum adsorption at equilibrium is 96% for 30 mg/l and the minimum 80% for 100 mg/l.
- The effect of concentration for adsorbent doses of 2, 4, 6, 8, and 10 g/l is shown in Fig. 8. As concentration increases from 10 to 100 mg/l, the percentage adsorption decreases and maximum adsorption is 96% for 10 g/l and minimum 80% for 2 g/l at an initial feed concentration of 10 mg/l.
- The pH of adsorbate solution has great effect on adsorption as shown in Fig. 9 and maximum adsorption was found at pH 1 for 30, 50, and 100 mg/l.
- The effect of particle size for 110, 60 and 30 mm mesh size is shown in Fig. 10. As size increases the adsorption decreases and for 110 mm mesh size, the maximum adsorption was 96% and minimum 60% at 10 mg/l.
- The equilibrium data for doses of 1, 2, 3, 4 and 5 g/l was tried to fit in Lagergren and pseudo-second-order model. The value of correlation coefficient (R^2) was calculated from Figs. 14 and 15 and found that both models fitted the equilibrium data.
- The Webber and Morris model also fits the equilibrium data and the coefficient of correlation was calculated from Fig. 13 which is 0.97333, 0.96846, 0.94608, 0.79266, and 0.92475 for1, 2, 3, 4, and 5 g/l.
- Langmuir and Freundlich isotherm was used for fitting of equilibrium data at a concentration of 30 mg/l and is shown in Figs. 11 and 12. The correlation coefficient (R^2) was 0.9624 for Langmuir and 0.9557 for Freundlich isotherm, and the maximum adsorption capacity was 22.96 mg/g.

Acknowledgement

The authors gratefully acknowledge the support for this work by National Research Foundation (NRF) of South Africa (Ref: IFR2011032900004).

References

[1] J.K. Acharya, J.N. Sahu, B.K. Sahoo, C.R. Mohanty, B.C. Meikap, Removal of Cr(VI) from waste water by activated carbon developed from tamarind wood activated with zinc chloride, J. Chem. Eng. 150 (2009) 25–39.

[2] K. Mohanty, M. Jha, B.C. Meikap, M.N. Biswas, Removal of Cr(VI) from dilute aqueous solution by activated carbon developed from Terminalia Arjun nut activated with zinc chloride, Chem. Eng. J. 60 (2005) 3039–3059.

[3] X.S. Wang, L.F. Chen, F.Y. Li, K.L. Chen, W.Y. Wan, Y.J. Tang, Removal of Cr(VI) with wheat-residue derived black carbon: Reaction mechanism and adsorption performance, J. Hazard. Mater. 175 (2010) 816–822.

[4] H. Zhang, Yi Tang, Dongqing Cai, Xianan Liu, Xiangqin Wang, Qing Huang, Zengliang Yu, Hexavalent chromium removal from aqueous solution by algal bloom residue derived activated carbon: Equilibrium and kinetic studies, J. Hazard. Mater. 181 (2010) 801–808.

[5] D.M. Khamis, M. Manassra, A. Mer'eb, Selective adsorption of chromium(VI) in industrial wastewater using low-cost abundantly available adsorbents. Adv. Environ Res. 6 (2002) 533–540.

[6] F.N. Acar, E. Malkoc, The removal of chromium(VI) from aqueous solutions by *Fagus orientalis* L, Bioresour. Technol. 94 (2004) 13–15.

[7] A.E. Sikaily, A.E. Nemr, A. Khaled, O. Abdelwehab, Removal of toxic chromium from wastewater using green alga *Ulva lactuca* and its activated carbon, J. Hazard. Mater. 148 (2007) 216–228.

[8] A. Ayuso, E. Garcia-Sanchez, A. Querol, Adsorption of Cr(VI) from synthetic solutions and electroplating wastewaters on amorphous aluminium oxide, J. Hazard. Mater. 142 (2007) 191–198.

[9] H. Li, Z. Li, T. Liu, X. Xiao, Z. Peng, L. Deng, A novel technology for biosorption and recovery hexavalent chromium in wastewater by bio-functional magnetic beads, Bioresour. Technol. 99 (2002) 6271–6279.

[10] J. Laine, A. Calafat, Preparation and characterization of activated carbon from coconut shell impregnated with phosphoric acid, Chem. Eng. J. 27 (1989) 191–195.

[11] J. Wu, H. Zhang, P.J. He, Q. Yao, L.M. Shao, Chromium(VI) removal from aqueous solution by dried activated sludge biomass, J. Hazard. Mater. 176 (2010) 697–703.

[12] L. Dupont, E. Guillon, Removal of hexavalent chromium with a lignocellulosic substrate extracted from wheat bran, Environ. Sci. Technol. 37 (2003) 4235–4241.

[13] M.E. Nuhoglu, Potential of tea factory waste for Chromium (VI) removal from aqueous solutions: Thermodynamic and kinetic studies, Sep. Purif. Technol. 54 (2003) 291–298.

[14] O.S. Bello, Mohd Azmier Ahmad, Coconut shell based activated carbon for the removal of Malachite Green Dye from aqueous solution, Sep. Sci. Technol. 47 (2012) 903–912.

[15] S. Gupta, B.V. Babu, Removal of toxic metal Cr(VI) from aqueous solution using sawdust as adsorbent, J. Chem. Eng. 150 (2009) 352–365.

[16] W. Sousa Francisco, Green coconut shells applied as adsorbent for removal of toxic metal ions using fixed-bed column technology, J. Environ. Manage. 91 (2010) 1634–1640.